

Radiation-intensity and temperature dependence of microwave-induced magnetoresistance oscillations in high-mobility two-dimensional electron systems

X.L. Lei

Department of Physics, Shanghai Jiaotong University, 1954 Huashan Road, Shanghai 200030, China

We present a detailed theoretical investigation on the radiation induced giant magnetoresistance oscillations recently discovered in high-mobility two-dimensional electron gas. Electron interactions with impurities, transverse and longitudinal acoustic phonons in GaAs-based heterosystems are considered simultaneously. Multiphoton-assisted impurity scatterings are shown to be the primary origin of the resistance oscillation. Based on the balance-equation theory developed for magnetotransport in Faraday geometry, we are able not only to reproduce the observed period, phase and the negative resistivity of the main oscillations, but also to predict the secondary peak/valley structures relating to two-photon and three-photon processes. The dependence of the magnetoresistance oscillation on microwave intensity, the role of dc bias current and the effect of elevated electron temperature are discussed. Furthermore, we propose that the temperature-dependence of the resistance oscillation stems from the growth of the Landau level broadening due to the enhancement of acoustic phonon scattering with increasing lattice temperature. The calculated temperature-variation of the oscillation agrees well with experimental observations.

PACS numbers: 73.50.Jt, 73.40.-c, 78.67.-n, 78.20.Ls

I. INTRODUCTION

Tremendous interest in magneto-transport in two-dimensional electron system (2DES) has recently revived since the experimental discovery of giant oscillations of the longitudinal resistance as a function of the magnetic field in high mobility two-dimensional (2D) electron gas (EG) subjected to a microwave radiation,^{1,2,3} particularly following the recent observations of "zero-resistance" states in very clean samples by two independent groups.^{4,5,6,7} These radiation-induced oscillations of the longitudinal magnetoresistivity R_{xx} are periodic in inverse magnetic field $1/B$ but, unlike the well-known Shubnikov-de Haas (SdH) oscillation whose period is controlled by the electron density N_e ,⁸ their periods are determined by the radiation frequency ω . The observed R_{xx} oscillations exhibit a smooth magnetic-field variation with the resistivity maxima at $\omega/\omega_c = j - \delta_-$ and minima at $\omega/\omega_c = j + \delta_+$ (ω_c is the cyclotron frequency, $j = 1, 2, 3, \dots$) having positive δ_{\pm} ranging around $0.1 - 0.25$.^{4,7} The resistivity minimum goes downward with increasing sample mobility and/or increasing radiation intensity until a vanishing resistance state shows up, while the Hall resistivity keeps the classical form $R_{xy} = B/eN_e$ with no sign of quantum Hall plateau over the whole magnetic field range exhibiting R_{xx} oscillation. Later independent experiments^{9,10} confirmed these results and the corresponding zero-conductance states were also observed in the Corbino samples.¹¹

To explore the origin of these peculiar "zero-resistance" states, different mechanisms have been suggested.^{12,13,14,15,16,17} As is shown by Andreev *et al.*¹³ that a negative linear conductance implies that the zero current state is intrinsically unstable: the system spontaneously develops a non-vanishing local current density which is determined by the condition that the component of electric field parallel to the local current vanishes.

Thus the appearance of negative longitudinal resistivity or conductivity in a uniform model suffices to explain the observed vanishing resistance. The possibility of absolute negative photoconductance in a 2DES subject to a perpendicular magnetic field was first explored 30 years ago by Ryzhii.^{18,19} Experimentally Keay *et al.*²⁰ reported the observation of absolute negative conductance in sequential resonant tunneling superlattices driven by intense terahertz radiation. Recent works^{12,14,15} indicated that the periodical structure of the density of states (DOS) of the 2DEG in a magnetic field and the photon-excited electron scatterings by impurities are the main origin of the magnetoresistance oscillations. Durst *et al.*¹² proposed a microscopic analysis for the conductivity assuming a δ -correlated disorder and a simple form of the 2D electron self-energy oscillatory with the magnetic field, obtaining the correct period, phase and the possible negative resistivity. Shi and Xie¹⁵ gave a similar result using the Tien and Gordon current formula²¹ for photon-assisted coherent tunneling. A more quantitative theoretical description was reported recently using a balance equation approach developed for radiation-induced magnetotransport in Faraday geometry,²² not only reproducing the correct period, phase and the negative resistivity of the main oscillations, but also predicting the secondary peaks and additional maxima and minima observed in the experiment,^{4,5,7,9} and identifying them as arising from double- and triple-photon processes. A quantum Boltzmann equation approach based on self-consistent Born approximation for large filling factors has also been presented very recently, taking account of the elastic (impurity) scattering as the major mechanism for radiation-induced magnetoresistance oscillation.²³ In addition to photon-assisted impurity scattering referred above as the mechanism of the absolute negative conductivity (ANC), other possible mechanisms were also explored in the literature. Ryzhii *et al.* proposed that acoustic phonon

scattering^{24,25} and heating of electrons²⁶ could also serve as the mechanisms of ANC in 2DES, and made a further attempt to connect them with experiments.²⁷

One of the most important and interesting features of this phenomenon is its sensitive temperature dependence. The "zero-resistance" states and radiation-induced magnetoresistance oscillations show up strongly only at low temperatures typically around $T = 1$ K or lower. At fixed microwave power with increasing temperature, not only the zero-resistance regions become narrower and eventually disappear, the whole oscillatory structure (peaks and valleys) diminish as well. At temperature $T \geq 4$ -5 K, oscillatory structure disappears completely and the resistivity R_{xx} -versus-magnetic field becomes essentially structureless.^{4,5} The temperature-variation of R_{xx} at deepest minima exhibits approximate activated-type behavior $\exp(T_0/T)$. However, the activation energies observed by both groups are very high: up to 10 K and 20 K at $j = 1$ minimum respectively.^{4,5} These values are about an order of magnitude higher than the microwave photon energy ($\omega \sim 3$ -5 K) and Landau-level spacing ($\omega_c \leq 2$ K). Furthermore, different T_0 values observed by the two groups indicate that the disappearing speed of the oscillatory structure with increasing temperature is sample dependent.^{4,5} To my knowledge, there has been no theoretical attempt to explain this temperature dependence, except that a conjecture of the formation of an energy gap around the Fermi surface is suggested under microwave irradiation around the resistance minima.⁴

The recently constructed balance-equation model,^{22,28} which provides a quantitative and tractable approach to radiation-induced magnetotransport in Faraday geometry, enables us not only to analyze the magnetoresistance oscillation, its dependence on the radiation intensity, but also to deal with its temperature variation in a comprehensive way. We suggest that the temperature suppression of the magnetoresistance oscillation in these high-mobility 2DES comes mainly from the growth of the Landau level broadening due to the rapid enhancement of acoustic phonon scatterings with increasing temperature at this low temperature range.

In this paper we will carry out a detailed theoretical investigation on the different aspects of radiation-induced magnetoresistance oscillation. The paper is organized as follows. For the convenience and completeness we present the general theoretical model and formulation in Section II. As a typical example we analyze GaAs-based systems for which the relevant material parameters are discussed in the Section III. Section IV concentrates on the transport properties of GaAs-based heterosystems at lattice temperature $T = 1$ K. We will give a detailed discussion on the impurity and acoustic phonon scattering related linear and nonlinear magnetoresistance induced by the irradiation of 0.1 THz microwave of different intensities, and the effect of elevated electron temperature. Section V is devoted to the analyses on the lattice-temperature dependence of the magnetoresistance oscillation. Finally, a brief summary is given in Section VI.

II. FORMULATION

A. Balance equations in crossed electric and magnetic fields

The experiments allow us to assume the 2DEG being in extended states over the magnetic field range relevant to this phenomenon. For a general treatment, we consider N_e electrons in a unit area of a quasi-2D system in the x - y plane with a confining potential $V(z)$ in the z -direction. These electrons, besides interacting with each other, are scattered by random impurities/disorders and by phonons in the lattice. To include possible elliptically polarized microwave illumination we assume that a uniform dc electric field \mathbf{E}_0 and a high-frequency (HF) ac field of frequency ω ,

$$\mathbf{E}_t \equiv \mathbf{E}_s \sin(\omega t) + \mathbf{E}_c \cos(\omega t), \quad (1)$$

are applied in the x - y plane, together with a magnetic field $\mathbf{B} = (0, 0, B)$ along the z direction. In terms of the 2D center-of-mass momentum and coordinate of the electron system,^{29,30,31} which are defined as $\mathbf{P} \equiv \sum_j \mathbf{p}_{j\parallel}$ and $\mathbf{R} \equiv N_e^{-1} \sum_j \mathbf{r}_{j\parallel}$ with $\mathbf{p}_{j\parallel} \equiv (p_{jx}, p_{jy})$ and $\mathbf{r}_{j\parallel} \equiv (x_j, y_j)$ being the momentum and coordinate of the j th electron in the 2D plane, and the relative electron momentum and coordinate $\mathbf{p}'_{j\parallel} \equiv \mathbf{p}_{j\parallel} - \mathbf{P}/N_e$ and $\mathbf{r}'_{j\parallel} \equiv \mathbf{r}_{j\parallel} - \mathbf{R}$, the Hamiltonian of the system can be written as the sum of a center-of-mass part H_{cm} and a relative electron part H_{er} ($\mathbf{A}(\mathbf{r})$ is the vector potential of the \mathbf{B} field),

$$\begin{aligned} H_{\text{cm}} &= \frac{1}{2N_e m} (\mathbf{P} - N_e e \mathbf{A}(\mathbf{R}))^2 - N_e e (\mathbf{E}_0 + \mathbf{E}_t) \cdot \mathbf{R}, \quad (2) \\ H_{\text{er}} &= \sum_j \left[\frac{1}{2m} \left(\mathbf{p}'_{j\parallel} - e \mathbf{A}(\mathbf{r}'_{j\parallel}) \right)^2 + \frac{p_{jz}^2}{2m_z} + V(z_j) \right] \\ &\quad + \sum_{i < j} V_c(\mathbf{r}'_{i\parallel} - \mathbf{r}'_{j\parallel}, z_i, z_j), \quad (3) \end{aligned}$$

together with electron-impurity and electron-phonon interactions H_{ei} and H_{ep} . Here m and m_z are respectively the electron effective mass parallel and perpendicular to the plane, and V_c stands for the electron-electron Coulomb interaction. It should be noted that the uniform electric field (dc and ac) appears only in H_{cm} , and that H_{er} is just the Hamiltonian of a quasi-2D system subjected to a magnetic field. The coupling between the center-of-mass and the relative electrons exists via the electron-impurity and electron-phonon interactions. Our treatment starts with the Heisenberg operator equations for the rates of changes of the center-of-mass velocity $\dot{\mathbf{V}} = -i[\mathbf{V}, H] + \partial \mathbf{V} / \partial t$, with $\mathbf{V} = -i[\mathbf{R}, H]$, and of the relative electron energy $\dot{H}_{\text{er}} = -i[H_{\text{er}}, H]$, and proceeds with the determination of their statistical averages.

As proposed in Ref. 29, the center-of-mass coordinate \mathbf{R} and velocity \mathbf{V} can be treated classically, i.e. as the time-dependent expectation values of the center-of-mass coordinate and velocity, $\mathbf{R}(t)$ and $\mathbf{V}(t)$, such that

$\mathbf{R}(t) - \mathbf{R}(t') = \int_{t'}^t \mathbf{V}(s) ds$. We are concerned with the steady transport state under an irradiation of single frequency and focus on the photon-induced dc resistivity and the energy absorption of the HF field. These quantities are directly related to the time-averaged and/or base-frequency oscillating components of the center-of-mass velocity. Although higher harmonics of the current may affect the dc and lower harmonic terms of the drift velocity through entering the damping force and energy exchange rates in the resulting equations, in an ordinary semiconductor the power of even the third harmonic current is rather weak as compared to the fundamental. For the HF field intensity in the experiments, the effect of higher harmonic current is safely negligible. Hence, it suffices to assume that the center-of-mass velocity, i.e. the electron drift velocity, consists of a dc part \mathbf{v}_0 and a stationary time-dependent part $\mathbf{v}(t)$ of the form

$$\mathbf{V}(t) = \mathbf{v}_0 + \mathbf{v}_1 \cos(\omega t) + \mathbf{v}_2 \sin(\omega t). \quad (4)$$

With this, the exponential factor in the operator equations can be expanded in terms of Bessel functions $J_n(x)$:

$$e^{-i\mathbf{q} \cdot \int_{t'}^t \mathbf{V}(s) ds} = \sum_{n=-\infty}^{\infty} J_n^2(\xi) e^{i(\mathbf{q} \cdot \mathbf{v}_0 - n\omega)(t-t')} + \sum_{m \neq 0} e^{im(\omega t - \varphi)} \sum_{n=-\infty}^{\infty} J_n(\xi) J_{n-m}(\xi) e^{i(\mathbf{q} \cdot \mathbf{v}_0 - n\omega)(t-t')}.$$

Here the argument in the Bessel functions

$$\xi \equiv \frac{1}{\omega} [(\mathbf{q}_{\parallel} \cdot \mathbf{v}_1)^2 + (\mathbf{q}_{\parallel} \cdot \mathbf{v}_2)^2]^{\frac{1}{2}} \quad (5)$$

and $\tan \varphi = (\mathbf{q} \cdot \mathbf{v}_2)/(\mathbf{q} \cdot \mathbf{v}_1)$. On the other hand, for 2D systems having electron sheet density of order of 10^{15} m^{-2} , the intra-band and inter-band Coulomb interactions are sufficiently strong that it is adequate to describe the relative-electron transport state using a single electron temperature T_e . Except this, the electron-electron

interaction is treated only in a mean-field level under random phase approximation (RPA).^{29,30} For the determination of unknown parameter \mathbf{v}_0 , \mathbf{v}_1 , \mathbf{v}_2 , and T_e , it suffices to know the damping force up to the base frequency oscillating term $\mathbf{F}(t) = \mathbf{F}_0 + \mathbf{F}_s \sin(\omega t) + \mathbf{F}_c \cos(\omega t)$, and the energy-related quantities up to the time-average term. We finally obtain the force and energy balance equations:

$$0 = N_e e \mathbf{E}_0 + N_e e (\mathbf{v}_0 \times \mathbf{B}) + \mathbf{F}_0, \quad (6)$$

$$\mathbf{v}_1 = \frac{e \mathbf{E}_s}{m\omega} + \frac{\mathbf{F}_s}{N_e m\omega} - \frac{e}{m\omega} (\mathbf{v}_2 \times \mathbf{B}), \quad (7)$$

$$-\mathbf{v}_2 = \frac{e \mathbf{E}_c}{m\omega} + \frac{\mathbf{F}_c}{N_e m\omega} - \frac{e}{m\omega} (\mathbf{v}_1 \times \mathbf{B}), \quad (8)$$

$$N_e e \mathbf{E}_0 \cdot \mathbf{v}_0 + S_p - W = 0. \quad (9)$$

Here

$$\begin{aligned} \mathbf{F}_0 &= \sum_{\mathbf{q}_{\parallel}} |U(\mathbf{q}_{\parallel})|^2 \sum_{n=-\infty}^{\infty} \mathbf{q}_{\parallel} J_n^2(\xi) \Pi_2(\mathbf{q}_{\parallel}, \omega_0 - n\omega) \\ &+ \sum_{\mathbf{q}} |M(\mathbf{q})|^2 \sum_{n=-\infty}^{\infty} \mathbf{q}_{\parallel} J_n^2(\xi) \Lambda_2(\mathbf{q}, \omega_0 + \Omega_{\mathbf{q}} - n\omega), \end{aligned} \quad (10)$$

is the time-averaged damping force, S_p is the time-averaged rate of the electron energy-gain from the HF field, $\frac{1}{2} N_e e (\mathbf{E}_s \cdot \mathbf{v}_2 + \mathbf{E}_c \cdot \mathbf{v}_1)$, which can be written in a form obtained from the right hand side of Eq. (10) by replacing the \mathbf{q}_{\parallel} factor with $n\omega$, and W is the time-averaged rate of the electron energy-loss due to coupling with phonons, whose expression can be obtained from the second term on the right hand side of Eq. (10) by replacing the \mathbf{q}_{\parallel} factor with $\Omega_{\mathbf{q}}$, the energy of a wavevector- \mathbf{q} phonon. The oscillating frictional force amplitudes $\mathbf{F}_s \equiv \mathbf{F}_{22} - \mathbf{F}_{11}$ and $\mathbf{F}_c \equiv \mathbf{F}_{21} + \mathbf{F}_{12}$ are given by ($\mu = 1, 2$)

$$\mathbf{F}_{1\mu} = - \sum_{\mathbf{q}_{\parallel}} \mathbf{q}_{\parallel} \eta_{\mu} |U(\mathbf{q}_{\parallel})|^2 \sum_{n=-\infty}^{\infty} [J_n^2(\xi)]' \Pi_1(\mathbf{q}_{\parallel}, \omega_0 - n\omega) - \sum_{\mathbf{q}} \mathbf{q}_{\parallel} \eta_{\mu} |M(\mathbf{q})|^2 \sum_{n=-\infty}^{\infty} [J_n^2(\xi)]' \Lambda_1(\mathbf{q}, \omega_0 + \Omega_{\mathbf{q}} - n\omega), \quad (11)$$

$$\mathbf{F}_{2\mu} = \sum_{\mathbf{q}_{\parallel}} \mathbf{q}_{\parallel} \frac{\eta_{\mu}}{\xi} |U(\mathbf{q}_{\parallel})|^2 \sum_{n=-\infty}^{\infty} 2n J_n^2(\xi) \Pi_2(\mathbf{q}_{\parallel}, \omega_0 - n\omega) + \sum_{\mathbf{q}} \mathbf{q}_{\parallel} \frac{\eta_{\mu}}{\xi} |M(\mathbf{q})|^2 \sum_{n=-\infty}^{\infty} 2n J_n^2(\xi) \Lambda_2(\mathbf{q}, \omega_0 + \Omega_{\mathbf{q}} - n\omega). \quad (12)$$

In these expressions, $\eta_{\mu} \equiv \mathbf{q}_{\parallel} \cdot \mathbf{v}_{\mu} / \omega \xi$; $\omega_0 \equiv \mathbf{q}_{\parallel} \cdot \mathbf{v}_0$; $U(\mathbf{q}_{\parallel})$ and $M(\mathbf{q})$ stand for effective impurity and phonon scattering potentials, $\Pi_2(\mathbf{q}_{\parallel}, \Omega)$ and $\Lambda_2(\mathbf{q}, \Omega) = 2\Pi_2(\mathbf{q}_{\parallel}, \Omega)[n(\Omega_{\mathbf{q}}/T) - n(\Omega/T_e)]$ (with $n(x) \equiv 1/(e^x - 1)$) are the imaginary parts of the electron density correlation function and electron-phonon correlation function in the

presence of the magnetic field. $\Pi_1(\mathbf{q}_{\parallel}, \Omega)$ and $\Lambda_1(\mathbf{q}, \Omega)$ are the real parts of these two correlation functions.

The HF field enters through the argument ξ of the Bessel functions in \mathbf{F}_0 , $\mathbf{F}_{\mu\nu}$, W and S_p . Compared with that without the HF field ($n = 0$ term only),³² we see that in an electron gas having impurity and/or phonon

scattering (otherwise homogeneous), a HF field of frequency ω opens additional channels for electron transition: an electron in a state can absorb or emit one or several photons and scattered to a different state with the help of impurities and/or phonons. The sum over $|n| \geq 1$ represents contributions of single and multiple photon processes of frequency- ω photons. These photon-assisted scatterings help to transfer energy from the HF field to the electron system (S_p) and give rise to additional damping force on the moving electrons.

Eqs. (6)-(9) form a closed set of equations for the determination of parameters \mathbf{v}_0 , \mathbf{v}_1 , \mathbf{v}_2 and T_e when \mathbf{E}_0 , \mathbf{E}_c and \mathbf{E}_s are given in a 2D system subjected to a magnetic field B at temperature T . Thus they provide a comprehensive and quantitative description of transport and optical properties of magnetically-biased quasi-2D semiconductors subjected to a dc bias and a HF radiation field in Faraday geometry.

Note that \mathbf{v}_1 and \mathbf{v}_2 always exhibit cyclotronresonance in the range $\omega \sim \omega_c$, as can be seen from Eqs. (7) and (8) rewritten in the form

$$\mathbf{v}_1 = \frac{\omega^2}{(\omega^2 - \omega_c^2)} \left\{ \frac{e}{m\omega} [\mathbf{E}_s + \frac{e}{m\omega} (\mathbf{E}_c \times \mathbf{B})] + \frac{1}{N_e m \omega} [\mathbf{F}_s + \frac{e}{m\omega} (\mathbf{F}_c \times \mathbf{B})] \right\}, \quad (13)$$

$$\mathbf{v}_2 = \frac{\omega^2}{(\omega_c^2 - \omega^2)} \left\{ \frac{e}{m\omega} [\mathbf{E}_c - \frac{e}{m\omega} (\mathbf{E}_s \times \mathbf{B})] + \frac{1}{N_e m \omega} [\mathbf{F}_c - \frac{e}{m\omega} (\mathbf{F}_s \times \mathbf{B})] \right\}. \quad (14)$$

Therefore, the argument ξ may be significantly different from that of the corresponding Bessel functions in the case without a magnetic field or with a magnetic field in Voigt configuration, where the electron motion is not affected by the magnetic field.³² On the other hand, impurity and phonon scatterings can affect ξ through the damping forces \mathbf{F}_s and \mathbf{F}_c . Eqs. (13) and (14) when neglecting the damping forces $\mathbf{F}_s = 0 = \mathbf{F}_c$, yield a Bessel-function argument ξ equivalent to that used in the early literature^{33,34}. The approximation of neglecting damping forces is valid only in weak scattering limit and away from cyclotronresonance. Depending on \mathbf{v}_1 and \mathbf{v}_2 , the damping forces \mathbf{F}_s and \mathbf{F}_c in Eqs. (13) and (14) are important not only in the general scattering case over the whole magnetic-field range but also in weak scattering case in the vicinity of cyclotron resonance in that they remove the divergence and yield finite oscillation velocities \mathbf{v}_1 and \mathbf{v}_2 at $\omega = \omega_c$.

B. Longitudinal and transverse resistivities

The nonlinear resistivity in the presence of a high-frequency field is easily obtained from Eq. (6). Taking \mathbf{v}_0 to be in the x direction, $\mathbf{v}_0 = (v_{0x}, 0, 0)$, we immedi-

ately get the transverse and longitudinal resistivities

$$R_{xy} \equiv \frac{E_{0y}}{N_e e v_{0x}} = \frac{B}{N_e e}, \quad (15)$$

$$R_{xx} \equiv \frac{E_{0x}}{N_e e v_{0x}} = -\frac{F_0}{N_e^2 e^2 v_{0x}}. \quad (16)$$

We see that in the present model (with parabolic energy spectrum) the transverse resistivity R_{xy} remains the classical form, with no change in the presence of HF radiation and/or dc current. The longitudinal resistivity R_{xx} , on the other hand, can be strongly affected by the irradiation also by dc bias. The linear longitudinal resistivity is the weak dc current limit ($v_{0x} \rightarrow 0$):

$$R_{xx} = -\sum_{\mathbf{q}_{\parallel}} q_x^2 \frac{|U(\mathbf{q}_{\parallel})|^2}{N_e^2 e^2} \sum_{n=-\infty}^{\infty} J_n^2(\xi) \left. \frac{\partial \Pi_2}{\partial \Omega} \right|_{\Omega=n\omega} - \sum_{\mathbf{q}} q_x^2 \frac{|M(\mathbf{q})|^2}{N_e^2 e^2} \sum_{n=-\infty}^{\infty} J_n^2(\xi) \left. \frac{\partial \Lambda_2}{\partial \Omega} \right|_{\Omega=\Omega_{\mathbf{q}}+n\omega} \quad (17)$$

Note that although according to Eqs. (10), (16) and (17), the linear and nonlinear longitudinal magnetoresistivity R_{xx} can formally written as the sum of contributions from various individual scattering mechanisms, all the scattering mechanisms have to be taken into account simultaneously in solving the momentum- and energy-balance equations (7), (8) and (9) for \mathbf{v}_1 , \mathbf{v}_2 and T_e , which enter the Bessel functions and other parts in the expression of R_{xx} .

C. Landau-level broadening

In the present model the effects of interparticle Coulomb interactions are included in the electron complex density correlation function $\Pi(\mathbf{q}_{\parallel}, \Omega) = \Pi_1(\mathbf{q}_{\parallel}, \Omega) + i\Pi_2(\mathbf{q}_{\parallel}, \Omega)$, which, in the random phase approximation, can be expressed as

$$\Pi(\mathbf{q}_{\parallel}, \Omega) = \frac{\Pi_0(\mathbf{q}_{\parallel}, \Omega)}{\epsilon(\mathbf{q}_{\parallel}, \Omega)}, \quad (18)$$

where

$$\epsilon(\mathbf{q}_{\parallel}, \Omega) \equiv 1 - V(q_{\parallel}) \Pi_0(\mathbf{q}_{\parallel}, \Omega) \quad (19)$$

is the complex dynamical dielectric function,

$$V(q_{\parallel}) = \frac{e^2}{2\epsilon_0 \kappa q_{\parallel}} H(q_{\parallel}) \quad (20)$$

is the effective Coulomb potential with κ the dielectric constant of the material and $H(q_{\parallel})$ a 2D wavefunction-related overlapping integration,³⁰ $\Pi_0(\mathbf{q}_{\parallel}, \Omega) = \Pi_{01}(\mathbf{q}_{\parallel}, \Omega) + i\Pi_{02}(\mathbf{q}_{\parallel}, \Omega)$ is the complex density correlation function of the independent electron system in the presence of the magnetic field. With this dynamically screened density correlation function the

collective plasma modes of the 2DES are incorporated. Disregard these collective modes one can just use a static screening $\epsilon(\mathbf{q}_{\parallel}, 0)$ instead.

The $\Pi_{02}(\mathbf{q}_{\parallel}, \Omega)$ function of a 2D system in a magnetic field can be written in terms of Landau representation:³¹

$$\Pi_{02}(\mathbf{q}_{\parallel}, \Omega) = \frac{1}{2\pi l_B^2} \sum_{n,n'} C_{n,n'} (l_B^2 q_{\parallel}^2 / 2) \Pi_2(n, n', \Omega), \quad (21)$$

$$\begin{aligned} \Pi_2(n, n', \Omega) = & -\frac{2}{\pi} \int d\varepsilon [f(\varepsilon) - f(\varepsilon + \Omega)] \\ & \times \text{Im} G_n(\varepsilon + \Omega) \text{Im} G_{n'}(\varepsilon), \end{aligned} \quad (22)$$

where $l_B = \sqrt{1/|eB|}$ is the magnetic length,

$$C_{n,n+l}(Y) \equiv n![(n+l)!]^{-1} Y^l e^{-Y} [L_n^l(Y)]^2 \quad (23)$$

with $L_n^l(Y)$ the associate Laguerre polynomial, $f(\varepsilon) = \{\exp[(\varepsilon - \mu)/T_e] + 1\}^{-1}$ the Fermi distribution function, and $\text{Im} G_n(\varepsilon)$ is the imaginary part of the electron Green's function, or the DOS, of the Landau level n . The real part function $\Pi_{01}(\mathbf{q}_{\parallel}, \Omega)$ and corresponding $\Lambda_{01}(\mathbf{q}_{\parallel}, \Omega)$ function can be derived from their imaginary parts via the Kramers-Kronig relation.

In principle, to obtain the Green's function $\text{Im} G_n(\varepsilon)$, a self-consistent calculation has to be carried out from the Dyson equation for the self-energy with all the impurity, phonon and other scatterings included. The resultant G_n is generally a complicated function of the magnetic field, temperature, and Landau-level index n , also dependent on the relative strengths of different kinds of scatterings.^{35,36} In the present study we do not attempt a self-consistent calculation of $G_n(\varepsilon)$. Instead, we choose a Gaussian-type form³⁵ for the purpose of demonstrating the observed oscillations (ε_n is the energy of the n -th Landau level):

$$\text{Im} G_n(\varepsilon) = -\sqrt{\frac{\pi}{2\Gamma^2}} \exp\left[-\frac{(\varepsilon - \varepsilon_n)^2}{2\Gamma^2}\right] \quad (24)$$

with a broadening width giving by

$$\Gamma = \left(\frac{2e\omega_c\alpha}{\pi m\mu_0(T)}\right)^{1/2}, \quad (25)$$

where $\mu_0(T)$ is the linear mobility at temperature T in the absence of the magnetic field and $\alpha > 1$ is a semiempirical parameter to take account the difference of the transport scattering time determining the mobility $\mu_0(T)$, to which larger angle scattering contributes a heavier weight, from the single particle lifetime, to which scattering with small or large angle equally contributes.^{4,12,14}

III. GAAS-BASED 2DES

To contact with recent experiments, we focus our attention to two ultra high mobility two-dimensional electron systems of GaAs/AlGaAs heterostructure with same

electron sheet density $N_e = 3 \times 10^{11} \text{ cm}^{-2}$ but having linear mobility $\mu_0(1 \text{ K}) = 2.4 \times 10^7 \text{ cm}^2 \text{ V}^{-1} \text{ s}^{-1}$ and $\mu_0(1 \text{ K}) = 1.46 \times 10^7 \text{ cm}^2 \text{ V}^{-1} \text{ s}^{-1}$ respectively in the absence of the magnetic field. In GaAs/AlGaAs systems, phonon modes and electron-phonon couplings are well established.³⁰ We consider both transverse acoustic phonons (interacting with electrons via piezoelectric coupling), and longitudinal acoustic phonons (interacting with electrons via piezoelectric and deformation potential couplings). We assumed that the elastic scatterings are either due to the remote charged impurities which are locate a distance $s = 60 \text{ nm}$ away from the interface of the heterojunction in the barrier side, or due to background impurities which are evenly distributed throughout the GaAs region. The impurity densities are determined by the requirement that electron total linear mobility equals the giving value at temperature $T = 1 \text{ K}$. The relevant effective impurity scattering potentials $|U(\mathbf{q}_{\parallel})|^2$ and electron-phonon matrix elements $|M(\mathbf{q})|^2$ were discussed earlier.³⁰ The material and coupling parameters for the system are well defined and taken as: electron effective mass $m = 0.068 m_e$ (m_e is the free electron mass), transverse sound speed $v_{st} = 2.48 \times 10^3 \text{ m/s}$, longitudinal sound speed $v_{sl} = 5.29 \times 10^3 \text{ m/s}$, acoustic deformation potential $\Xi = 8.5 \text{ eV}$, piezoelectric constant $e_{14} = 1.41 \times 10^9 \text{ V/m}$, dielectric constant $\kappa = 12.9$, material mass density $d = 5.31 \text{ g/cm}^3$. The depletion layer charge number density is taken as $N_{dep} = 5 \times 10^{10} \text{ cm}^{-2}$.

In GaAs systems at low temperatures $\mu_0(T)$ comes from impurity, transverse and longitudinal acoustic phonon scatterings:

$$\frac{1}{\mu_0} = \frac{1}{\mu_0^{(i)}} + \frac{1}{\mu_0^{(pt)}} + \frac{1}{\mu_0^{(pl)}}. \quad (26)$$

The longitudinal magnetoresistivity R_{xx} can also be formally written as the sum of the impurity, transverse and longitudinal acoustic phonon contributions:

$$R_{xx} = R_{xx}^{(i)} + R_{xx}^{(pt)} + R_{xx}^{(pl)}. \quad (27)$$

In the following sections we will carried out numerical calculations for $R_{xx}^{(i)}$, $R_{xx}^{(pt)}$ and $R_{xx}^{(pl)}$ assuming linearly polarized MW fields ($\mathbf{E}_c = 0$) with multiphoton processes included.

The microwave field intensity required for the appearance of resistivity oscillation in these high-mobility samples is moderate. The slight electron heating induced by the irradiation in these systems is unimportant as far as the main phenomenon is concerned. As can be seen later that the radiation-induced magnetoresistance oscillation is not sensitive to the moderate rise of electron temperature. Therefore, R_{xx} can be obtained directly from Eq.(17) with $T_e = T$. We will check the effect of elevated electron temperature in the subsection IV-c.

IV. R_{xx} AT TEMPERATURE $T = 1$ K

A. Impurity-induced magnetoresistivity

1. Linear resistivity

We first assume that the elastic scatterings are due to ionized remote impurities.³⁰ Fig. 1a shows the impurity-induced longitudinal resistivity $R_{xx}^{(i)}$ versus $\omega/\omega_c \equiv \gamma_c$ subjected to a microwave radiation of frequency $\omega/2\pi = 0.1$ THz at four values of amplitude: $E_s = 20, 45, 65$ and 80 V/cm. At temperature $T = 1$ K SdH oscillations of period $\gamma_c = 0.039$ show up strongly at high ω_c side, and then gradually decay away as $1/\omega_c$ increases. In addition to this all four resistivity curves exhibit clear oscillation having the main oscillation period $\gamma_c = 1$ (they are crossing at integer points $\gamma_c = 2, 3, 4, 5$). The resistivity maxima locate around $\gamma_c = j - \delta_-$ and minima around $\gamma_c = j + \delta_+$ with $\delta_{\pm} \sim 0.22 - 0.26$ for $j = 3, 4, 5$, $\delta_{\pm} \sim 0.17 - 0.22$ for $j = 2$, and $\delta_{\pm} \sim 0.08 - 0.14$ for $j = 1$ (Fig. 1b). The amplitude of the oscillation increases with increasing HF field intensity for $\gamma_c > 1.5$. Resistivity gets into negative value for $E_s = 80$ V/cm around the minima at $j = 1, 2$ and 3 , for $E_s = 65$ V/cm at $j = 1$ and 2 , and for $E_s = 20$ and 45 V/cm at $j = 1$. These main peak-valley structures are related to single-photon ($|n| = 1$) processes. In the vicinity of $\gamma_c = 1$, where the cyclotron resonance greatly enhances the effective amplitude of the HF field in photon-assisted scatterings, multiphoton processes show up. The amplitudes of the $j = 1$ maximum and minimum no longer monotonically change with field intensity. Furthermore, there appears a shoulder around $\gamma_c = 1.5$ on the curves of $E_s = 45$ and 65 V/cm, and it develops into a secondary peak in the $E_s = 80$ V/cm case. This peak-valley structure around $\gamma_c = 1.5$ is related to two-photon ($|n| = 2$) processes. The oscillatory peak-valley structure related to three-photon processes was also demonstrated in the cases of lower microwave frequency ($\omega = 60$ and 40 GHz).²²

The dependence of the resistivity at maxima and minima on the microwave intensity is shown in Fig. 1c, where we plot the calculated photoresistivity, i.e. the magnetoresistivity in the presence of radiation, $R_{xx}^{(i)}$, minus the dark resistivity $R_{xx}(E_s = 0)$, as a function of radiation field amplitude E_s at peaks and valleys of $j = 2$ and $j = 3$. We see that $|R_{xx}^{(i)} - R_{xx}(0)|$ grows like E_s^2 at lower intensity and become linearly dependent on E_s at higher intensity within the amplitude range shown. This is in agreement with experiments.^{4,5,6}

Fig. 1d shows the positive parts of $R_{xx}^{(i)}/R_{xx}(E_s = 0)$ at minima of $j = 2, 3$ and 4 on logarithmic scale as functions of E_s^2 .

It should be noted that the above feature of impurity-induced magnetoresistivity is not very sensitive to the form of elastic scattering potential. In Fig. 2a we demonstrate $R_{xx}^{(i)}$ due to background impurity scattering as a function of ω/ω_c under several different microwave ampli-

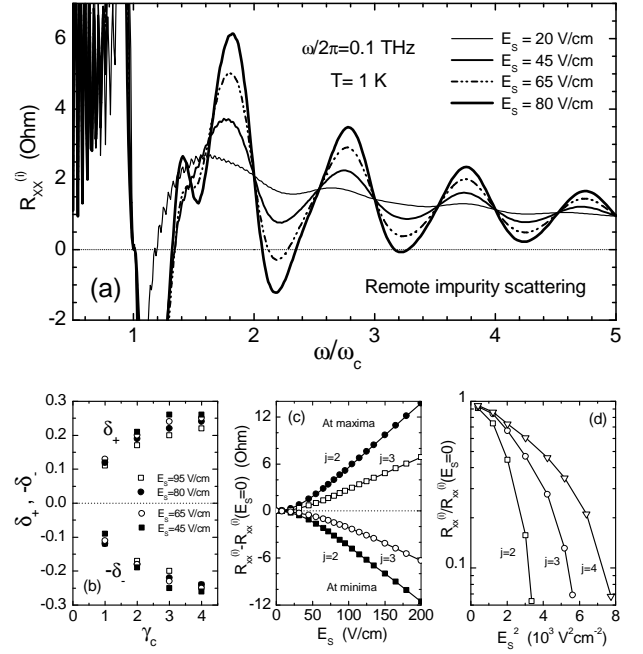


FIG. 1: (a) The longitudinal linear magnetoresistivity $R_{xx}^{(i)}$ induced by remote-impurity scattering in a GaAs-based heterosystem subjected to crossed magnetic fields B and in-plane linearly polarized HF fields $E_s \sin(\omega t)$ of frequency $\omega/2\pi = 0.1$ THz with several different amplitudes at lattice temperature $T = 1$ K. $\omega_c \equiv eB/m$ stands for the cyclotron frequency. The other parameters are: electron density $N_e = 3.0 \times 10^{11} \text{ cm}^{-2}$, zero-magnetic-field linear dc mobility $\mu_0(1 \text{ K}) = 2.4 \times 10^7 \text{ cm}^2 \text{ V}^{-1} \text{ s}^{-1}$, and the broadening coefficient $\alpha = 12$. The electron temperature is set to be $T_e = T$. (b) Parameters δ_+ and δ_- for locations of resistance maxima and minima at several HF field amplitudes. (c) The photoresistivity $R_{xx}^{(i)} - R_{xx}^{(i)}(E_s = 0)$ at maxima and at minima of $j = 1$ and $j = 2$ against the amplitude of the HF field. (d) $R_{xx}^{(i)}/R_{xx}^{(i)}(E_s = 0)$ is shown against E_s^2 on logarithmic scale for $j = 2, 3$ and 4 .

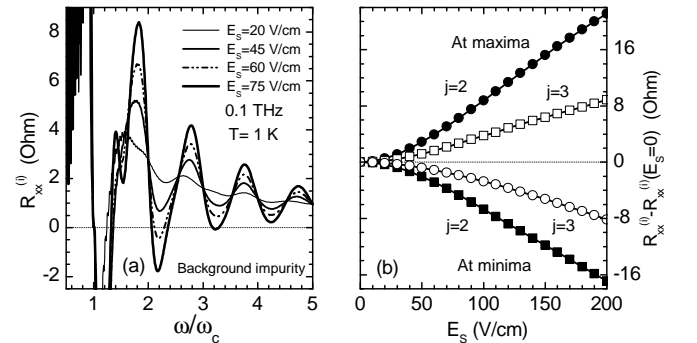


FIG. 2: (a) The linear magnetoresistivity $R_{xx}^{(i)}$ induced by background-impurity scattering in a GaAs-based 2DEG subjected to linearly polarized HF fields $E_s \sin(\omega t)$ of frequency $\omega/2\pi = 0.1$ THz. The system parameters are the same as indicated in Fig. 1. (b) The background impurity-induced photoresistivity $R_{xx}^{(i)} - R_{xx}^{(i)}(0)$ at maxima and at minima of $j = 1$ and $j = 2$ shown in Fig. 2a is plotted against the amplitude of the HF field.

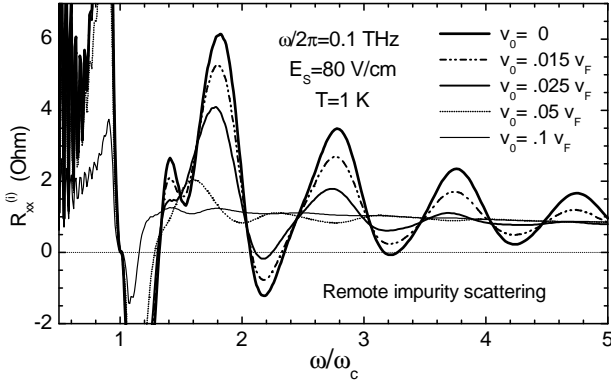


FIG. 3: Remote-impurity induced nonlinear longitudinal magnetoresistivity $R_{xx}^{(i)}$ as defined in Eq.(16) in the GaAs-based 2DEG subjected to crossed magnetic fields B and an in-plane linearly polarized HF field $E_s \sin(\omega t)$ of frequency $\omega/2\pi = 0.1$ THz and amplitude $E_s = 80$ V/cm under several different dc bias velocities $v_0 = 0, .015, .025, .05$ and $.1 v_F$, where $v_F = 2.4 \times 10^5$ m/s is the electron Fermi velocity. $\omega_c \equiv eB/m$ is the cyclotron frequency. The other parameters are the same as indicated in Fig. 1.

tudes. Although the scattering potential of background impurities appears quite different from that of remote impurities,³⁰ the main features of the radiation-induced magnetoresistivity oscillation are in common for both scattering potentials. The difference shows up only in some quantitative details. The dependence of the background impurity induced resistivity at maxima and minima on the microwave intensity shown in Fig. 2b, is also similar to the case of remote impurity scattering (Fig. 1c).

2. Nonlinear resistivity

Fig. 3 shows the nonlinear longitudinal resistivity $R_{xx}^{(i)}$ due to remote-impurity scattering calculated directly from Eq. (16) for the 2DES subject to a 0.1 THz microwave radiation of amplitude $E_s = 80$ V/cm under different dc bias velocities $v_0 = 0, .015, .025, .05$ and $0.1 v_F$, where the electron Fermi velocity $v_F = 2.4 \times 10^5$ m/s. For the given strength of the radiation field the linear magnetoresistivity (vanishing E_0 or v_0) exhibits the strongest oscillation. A finite dc bias always suppresses the oscillation and may destroy the negative resistivity appearing at vanishing dc bias.

B. Acoustic-phonon-induced magnetoresistivity

Acoustic phonon scattering has recently been proposed as a mechanism of the absolute negative resistivity leading to vanishing resistance state.^{24,25} To check such a possibility we show in Fig. 4 the linear magnetoresistivity R_{xx} , contributed separately by transverse acoustic phonon scattering (a) and by longitudinal acoustic phonon scattering (b), as functions of ω/ω_c under

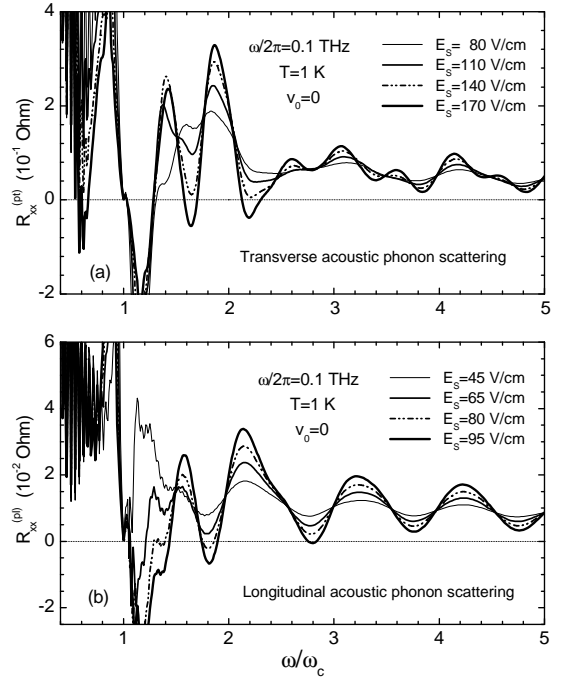


FIG. 4: Linear magnetoresistivities $R_{xx}^{(pt)}$ (a) and $R_{xx}^{(pl)}$ (b) induced by transverse and longitudinal acoustic phonons in a GaAs-based 2DES subjected to microwave fields $E_s \sin(\omega t)$ of frequency $\omega/2\pi = 0.1$ THz having different amplitudes. The lattice temperature is $T = 1$ K and the electron temperature $T_e = T$. The other parameters are: electron density $N_e = 3.0 \times 10^{11} \text{ cm}^{-2}$, dc mobility $\mu_0(1\text{K}) = 2.4 \times 10^7 \text{ cm}^2 \text{ V}^{-1} \text{ s}^{-1}$, and the broadening coefficient $\alpha = 12$.

0.1 THz microwave illumination of different strengths. Photon-assisted acoustic-phonon scattering itself indeed can give rise to pronounced resistance oscillation with changing magnetic field and R_{xx} at oscillation minima can go down to negative under sufficiently strong microwave irradiation for both transverse and longitudinal phonon scatterings. These acoustic-phonon induced R_{xx} oscillations, though can still be considered nearly periodic in inverse magnetic field, exhibit quite different behavior from that of impurity-induced R_{xx} oscillation shown in Fig. 1 and also different from each other, especially in respect to the phase of the oscillation. In the case of impurity scattering the resistance maxima always appear at $\gamma_c = j - \delta_-$ and the minima at $\gamma_c = j + \delta_+$, while in the case of longitudinal acoustic scattering the maxima appear at $\gamma_c = j + \delta_+$ and the minima at $\gamma_c = j - \delta_-$ except the case of $j = 1$. The phase of transverse acoustic phonon induced R_{xx} oscillation resembles that of impurity at $j = 1, 2$ but becomes that of longitudinal acoustic phonon at $j = 3, 4, 5$.

As in the case of impurity scattering a finite dc bias always suppresses the phonon-induced resistance oscillations and may destroy the negative resistivity appearing at vanishing dc bias as seen in Fig. 5, where we plot the nonlinear longitudinal resistivity $R_{xx}^{(pt)}$ induced by transverse acoustic phonons and $R_{xx}^{(pl)}$ induced by longitudi-

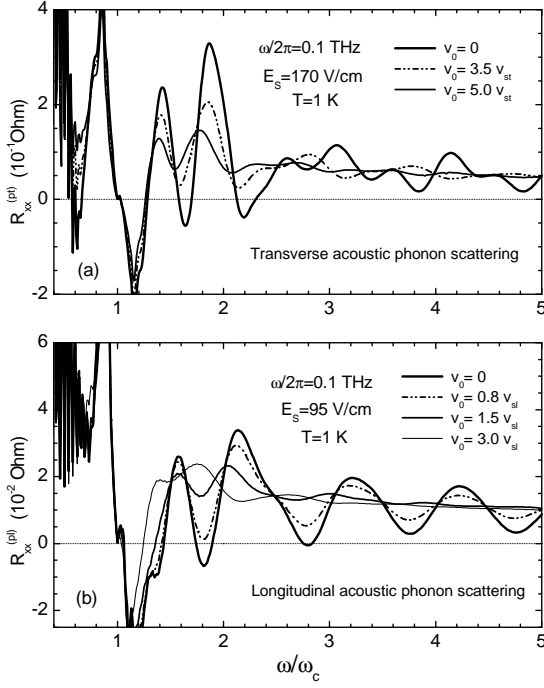


FIG. 5: Nonlinear magnetoresistivities $R_{xx}^{(pt)}$ (a) and $R_{xx}^{(pl)}$ (b) induced by transverse and longitudinal acoustic phonons under different dc bias v_0 in a GaAs-based 2DES exposed to microwave fields $E_s \sin(\omega t)$ of frequency $\omega/2\pi = 0.1$ THz having amplitude $E_s = 170$ V/cm and $E_s = 95$ V/cm respectively. Here $v_{st} = 2.48 \times 10^3$ m/s and $v_{sl} = 5.29 \times 10^3$ m/s are the transverse and longitudinal sound speed. The other parameters are the same as indicated in Fig. 4.

nal acoustic phonons, for the 2DEG subject to a 0.1 THz microwave radiation with fixed amplitudes under several different dc current biases. These results are in qualitative agreement with a recent report.³⁷

However, at temperature $T = 1$ K the acoustic phonon scattering contributes a part of R_{xx} which is more than an order of magnitude smaller than that contributed from impurity scattering in the system having a mobility of $2.4 \times 10^7 \text{ cm}^2 \text{ V}^{-1} \text{ s}^{-1}$ at $T = 1$ K. Therefore, acoustic phonon scattering essentially gives no direct contribution to the experimentally observed resistance oscillation at this low temperature. Nevertheless, acoustic phonons play a key role in suppressing the resistance oscillation at elevated lattice temperatures. We will discuss this issue in Section V.

C. Effect of elevated electron temperature

Upon the microwave irradiation the electron temperature can be higher than the lattice temperature. To have an idea of how the elevated electron temperature affects the magnetoresistivity oscillation we show in Fig. 6a the background impurity induced longitudinal resistivity $R_{xx}^{(i)}$ of the 2DEG having several different electron temperatures $T_e = 1, 5$ and 50 K but all at the same

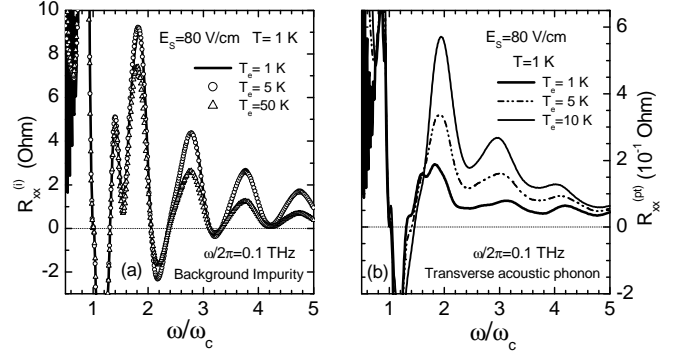


FIG. 6: The impurity-induced linear magnetoresistivity $R_{xx}^{(i)}$ (a) and transverse acoustic phonon induced linear magnetoresistivity $R_{xx}^{(pt)}$ of a GaAs-based 2DES subjected to a microwave field of amplitude $E_s = 80$ V/cm and frequency $\omega/2\pi = 0.1$ THz at elevated electron temperatures. The lattice temperature is $T = 1$ K. The other parameters are the same as indicated in Fig. 4.

lattice temperature $T = 1$ K subject to a microwave irradiation of frequency $\omega/2\pi = 0.1$ THz and amplitude $E_s = 80$ kV/cm. We see that at $T_e = 5$ K (even much lower) SdH oscillations disappear completely, but the radiation-induced oscillations remain essentially the same. Only when the electron temperature becomes much higher, e.g. 50 K, can appear the appreciable change in the resistance oscillation curve. This indicates that the radiation-induced resistivity oscillation is quite insensitive to electron temperature and we can analyze the moderate-strength microwave induced resistivity oscillation by neglecting the electron temperature change in the system. On the other hand, using a slightly elevated electron temperature provides a way to separate the radiation-induced oscillation from the SdH effect.

Fig. 6b shows the effect of elevated electron temperature on transverse acoustic phonon induced resistivity $R_{xx}^{(pt)}$. With electron temperature increasing from $T_e = 1$ K to 5 K, the magnitude of the oscillation somewhat grows. But its absolute contribution to magnetoresistivity is still an order of magnitude smaller than the of impurity as long as the lattice temperature remains $T = 1$ K.

Experiments showed that the strongest SdH oscillations always show up on the dark resistivity curve and with enhancing the radiation intensity the SdH oscillations weaken.^{4,6} This fact can be easily understood as due to the rise of the electron temperature caused by the microwave illumination: SdH oscillations are suppressed by the rising electron temperature, while the radiation-induced R_{xx} oscillations remain the same as long as the lattice temperature keeps unchange.

V. EFFECT OF ELEVATED LATTICE TEMPERATURE

One of the most important aspect of the experimental finding on the magnetoresistance oscillation in irradiated 2DES is the temperature-dependence of R_{xx} . Experiments^{4,5} found that the "zero-resistance" states and radiation-induced magnetoresistance oscillations show up strongly only at low temperatures typically around $T = 1$ K or lower. At fixed microwave power with increasing temperature, not only the zero-resistance regions become narrower and eventually disappear, the whole oscillatory structure (peaks and valleys) diminish as well. At temperature $T \geq 4.5$ K, oscillatory structure disappears completely and the resistivity R_{xx} -versus magnetic field becomes essentially flat.⁵

Both groups analyzed the temperature-variation of R_{xx} at deepest minima using an activated-type dependence $\exp(T_0/T)$. The activation energies observed by both groups are very high and different: up to 10 K and 20 K at $j = 1$ minimum respectively.^{4,5} These values are about an order of magnitude higher than the microwave photon energy ($\omega \sim 3$ -5 K) and Landau-level spacing ($\omega_c \leq 2$ K). The different T_0 values observed by the two groups indicate that the speed of the oscillatory structure disappearing with temperature is sample dependent.^{4,5} To explain the temperature dependence the formation of an energy gap around the Fermi surface in the spectrum is suggested under microwave irradiation around the resistance minima.⁴

Our explanation of the temperature dependence of the magnetoresistance oscillations is based on the temperature variation of the Landau level broadening Γ as determined by Eq. (25). In a GaAs-based system, when the lattice temperature increases from around $T = 1$ K, the numbers of transverse and longitudinal acoustic phonons and thus the electron-phonon scattering strengths increase rapidly. In Fig. 7b we plot the zero-magnetic-field linear mobility $\mu_0^{(pt)}$ due to transverse acoustic phonon scattering, $\mu_0^{(pl)}$ due to longitudinal phonon scattering, and the total mobility μ_0 as functions of lattice temperature T for the GaAs-based heterosystem with $\mu_0 = 2.4 \times 10^7 \text{ cm}^2 \text{ V}^{-1} \text{ s}^{-1}$ at $T = 1$ K. We see that when temperature T rises from 1 K to 3 K the phonon related mobilities decline about an order of magnitude, leading to the total mobility $\mu_0(T)$ decreasing about a factor of 2.2 and, according to (25), Γ increasing about a factor of 1.5 (assuming α unchanged). The temperature growth of the Landau-level width due to this enhanced phonon scattering results in the strong temperature variation of the radiation-induced magnetoresistance oscillation. The effect of such a mobility decrease or the Landau level broadening on R_{xx} is significant. Fig. 7a shows the calculated linear resistivity R_{xx} as a function of ω/ω_c at different lattice temperatures $T = 1.0, 1.5, 2.0, 2.5, 3.0, 3.5, 4.0$ and 4.5 K for the system of $\mu_0(1 \text{ K}) = 2.4 \times 10^7 \text{ cm}^2 \text{ V}^{-1} \text{ s}^{-1}$ under a fixed microwave illumination of frequency $\omega/2\pi = 0.1$ THz and

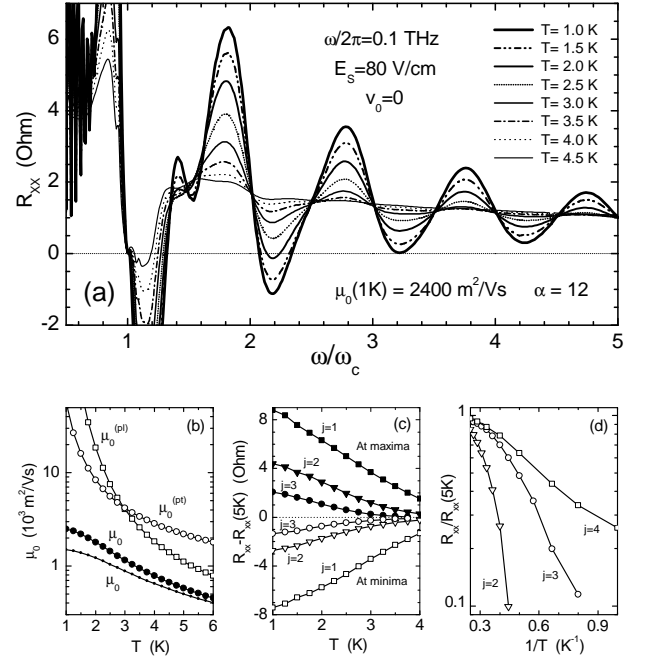


FIG. 7: (a) The longitudinal magnetoresistivity R_{xx} at different lattice temperatures $T = 1.0, 1.5, 2.0, 2.5, 3.0, 3.5, 4.0$ and 4.5 K for a GaAs-based 2DEG subjected to a HF field $E_s \sin(\omega t)$ of frequency $\omega/2\pi = 0.1$ THz and amplitude $E_s = 80$ V/cm. The system parameters are: electron density $N_e = 3.0 \times 10^{11} \text{ cm}^{-2}$, dc mobility $\mu_0 = 2.4 \times 10^7 \text{ cm}^2 \text{ V}^{-1} \text{ s}^{-1}$ at $T = 1$ K, and the broadening coefficient $\alpha = 12$ for all the curves. (b) Zero magnetic field linear mobility induced by transverse acoustic phonon scattering, $\mu_0^{(pt)}$, by longitudinal acoustic phonon scattering, $\mu_0^{(pl)}$, and the total mobility μ_0 , for the system with $\mu_0(1 \text{ K}) = 2.4 \times 10^7 \text{ cm}^2 \text{ V}^{-1} \text{ s}^{-1}$ (dots), and for system with $\mu_0(1 \text{ K}) = 1.46 \times 10^7 \text{ cm}^2 \text{ V}^{-1} \text{ s}^{-1}$ (solid line). (c) The amplitudes of the resistivity oscillation $R_{xx}(T) - R_{xx}(5 \text{ K})$ at maxima and at minima versus temperature T for $j = 1, 2$ and 3 . (d) $R_{xx}(T)/R_{xx}(5 \text{ K})$ is shown against $1/T$ on logarithmic scale for $j = 2, 3$ and 4 .

amplitude $E_s = 80$ V/cm. The broadening parameter is fixed to be $\alpha = 12$ for all the curves of different lattice temperatures, and the electron temperature is taken to equal to the lattice temperature in all the calculations in this section. The sensitive temperature dependence of the resistance oscillation is quite obvious. The magnitude of peaks and valleys of the oscillation diminish straightforward with increasing temperature from 1 K. At $T \geq 4.5$ K the oscillation structure almost disappear and R_{xx} exhibits quite a flat form with changing ω/ω_c for $\gamma_c \geq 1.6$.

Comparing Fig. 7a with Fig. 1a,³⁸ we see that the role of decreasing inverse temperature at fixed radiation intensity is somewhat similar to that of reducing microwave intensity at fixed temperature. This similarity, however, holds only within the range of $T \leq 4.5$ K when direct phonon contribution to R_{xx} is still less important than that of impurities. At higher temperature the direct phonon contribution may become dominant and the

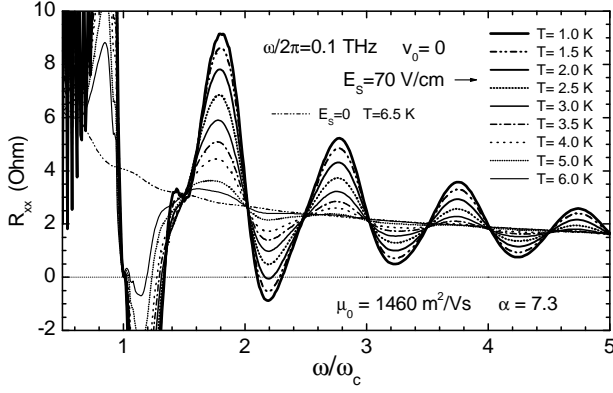


FIG. 8: The longitudinal magnetoresistivity R_{xx} at different lattice temperature $T = 1.0, 1.5, 2.0, 2.5, 3.0, 3.5, 4.0, 5.0$ and 6.0 K for a GaAs-based 2DEG subjected to a HF field $E_s \sin(\omega t)$ of frequency $\omega/2\pi = 0.1$ THz and amplitude $E_s = 70$ V/cm. The system parameters are: electron density $N_e = 3.0 \times 10^{11} \text{ cm}^{-2}$, dc mobility $\mu_0(1 \text{ K}) = 1.46 \times 10^7 \text{ cm}^2 \text{ V}^{-1} \text{ s}^{-1}$, and the broadening coefficient $\alpha = 7.3$ for all the curves. Also shown is the dark resistivity ($E_s = 0$) at $T = 6.5$ K.

structureless R_{xx} will continue to grow with rising T and the R_{xx} -vs- γ_c curves of different T will not cross at integer points $\gamma_c = 2, 3, 4, 5$, a feature of impurity scattering dominance.

To show the temperature variation of R_{xx} , we plot in Fig. 7c $R_{xx} - R_{xx}(5 \text{ K})$ at maxima and at minima of $j = 1, 2$ and 3 , as function of T . The oscillation disappears faster at larger j (lower magnetic field) than at smaller j (higher magnetic field). The positive values of $R_{xx}/R_{xx}(5 \text{ K})$ at peaks and at valleys also plotted against $1/T$ on logarithmic scale. If we roughly fit the data with the form $R_{xx}(T) \propto \exp(-T_0/T)$, we have $T_0 \approx 10 \text{ K}$ for $j = 2$, $T_0 \approx 4.5 \text{ K}$ for $j = 3$, and $T_0 \approx 2.1 \text{ K}$ for $j = 4$ in average over the range shown.

The sensitivity of the temperature variation of the radiation-induced magnetoresistance oscillation is sample dependent. In GaAs-based systems the electron-phonon scattering strengths, thus the acoustic-phonon induced mobilities $\mu_0^{(\text{pt})}$ and $\mu_0^{(\text{pl})}$ and their temperature behavior are essentially the same. Therefore, the temperature variation of the total mobility μ_0 depends mainly on the strength of the impurity scattering, which is almost temperature independent within this range of T . The lowest curve in fig. 7b shows the T -dependence of the total mobility $\mu_0(T)$ for the sample having $T = 1 \text{ K}$ mobility $\mu_0(1 \text{ K}) = 1.46 \times 10^7 \text{ cm}^2 \text{ V}^{-1} \text{ s}^{-1}$, which apparently exhibits a slower temperature change than that of $\mu_0(1 \text{ K}) = 2.4 \times 10^7 \text{ cm}^2 \text{ V}^{-1} \text{ s}^{-1}$ system.

In Fig. 8 we illustrate the linear resistivity R_{xx} as a function of ω/ω_c at different lattice temperatures $T = 1.0, 1.5, 2.0, 2.5, 3.0, 3.5, 4.0, 5.0$ and 6.0 K for the system of $\mu_0(1 \text{ K}) = 1.46 \times 10^7 \text{ cm}^2 \text{ V}^{-1} \text{ s}^{-1}$ under a fixed microwave irradiation of frequency $\omega/2\pi = 0.1$ THz and amplitude $E_s = 70$ V/cm. The broadening parameter is fixed to be $\alpha = 7.3$ for all the lattice temperatures.

The speed of the oscillatory structure disappearing with rising temperature is apparently slower than the system shown in Fig. 7a. We see that at $T \geq 6.0 \text{ K}$ the oscillation structure essentially disappear and R_{xx} approaches a flat form of dark ($E_s = 0$) curve of corresponding temperature (see Fig. 8) for $\gamma_c \geq 1.6$. Note that different from $T = 1 \text{ K}$ case, where impurity scattering dominates, at $T = 6 \text{ K}$ the acoustic phonon scatterings already yield a substantial contribution to both zero-field mobility μ_0 and to radiation-induced magnetoresistivity R_{xx} .

VI. CONCLUSION

Based on the balance-equation model for magneto-transport in Faraday geometry, we have carried out a detailed theoretical investigation on microwave-radiation induced magnetoresistance oscillations recently discovered in high-mobility GaAs-based two-dimensional electron systems. We find that for systems having zero-field linear mobility $\mu_0(1 \text{ K}) \leq 2.4 \times 10^7 \text{ cm}^2 \text{ V}^{-1} \text{ s}^{-1}$ multiphoton-assisted impurity scatterings are the main mechanisms responsible for radiation-induced magnetoresistance oscillations at temperature $T \leq 4 \text{ K}$. The amplitude of the R_{xx} oscillation grows roughly following the microwave power under weak illumination and following the microwave amplitude under medium illumination before it saturates even decreases with continuing increase of the microwave strength under strong irradiation. It is shown that the strongest oscillations appear in the linear longitudinal magnetoresistance and a finite dc current bias always suppresses the oscillation. We find that, different from the SdH oscillation which is easily suppressed by a few-degree rise of the electron temperature, the radiation-induced magnetoresistance oscillations are quite insensitive to the modest electron heating as long as the lattice temperature remain the same. Although the magnetoresistivities directly stemming from photon-assisted transverse and longitudinal acoustic phonon scatterings also exhibit pronounced oscillations under microwave irradiation, they contribute only a small part of the total R_{xx} in the temperature range of $T \leq 4 \text{ K}$. Nevertheless, as we proposed, that it is just this acoustic phonon scattering that gives rise to the sensitive lattice temperature dependence of radiation-induced resistance oscillations right from $T = 1 \text{ K}$. We showed that the growth of the Landau level broadening resulting from the enhancement of acoustic phonon scatterings with increasing lattice temperature leads to the observed temperature suppression of the oscillation.

Acknowledgments

The author is grateful to Dr. S.Y. Liu for helpful discussions, to Prof. V.I. Ryzhii for sending the information of Refs. 18,19,33,34. This work was supported by the National Science Foundation of China, the Special Funds for

-
- ¹ M.A. Zudov, R.R. Du, J.A. Simmons, and J.L. Reno, *Phys. Rev. B* **64**, 201311(R) (2001).
 - ² P.D. Ye, L.W. Engel, D.C. Tsui, J.A. Simmons, J.R. Wendt, G.A. Vawter, and J.L. Reno, *Appl. Phys. Lett.* **79**, 2193 (2001).
 - ³ R.G. Mani, J.H. Smet, K. von Klitzing, V. Narayanamurti, W.B. Johnson, and V. Umansky, preprint: cond-mat/0305507.
 - ⁴ R.G. Mani, J.H. Smet, K. von Klitzing, V. Narayanamurti, W.B. Johnson, and V. Umansky, *Nature* **420**, 646 (2002).
 - ⁵ M.A. Zudov, R.R. Du, L.N. Pfeiffer, and K.W. West, *Phys. Rev. Lett.* **90**, 046807 (2003).
 - ⁶ R.G. Mani, J.H. Smet, K. von Klitzing, V. Narayanamurti, W.B. Johnson, and V. Umansky, preprint: cond-mat/0306388.
 - ⁷ M.A. Zudov, preprint: cond-mat/0306508.
 - ⁸ W. Kohn, *Phys. Rev.* **123**, 1242 (1961).
 - ⁹ S.I. Dorozhkin, preprint: cond-mat/0304604.
 - ¹⁰ R.L. Willett, K.W. West, L.N. Pfeiffer, *Bull. Am. Phys. Soc.* **48**, 459 (2003).
 - ¹¹ C.L. Yang, M.A. Zudov, T.A. Knuuttila, and R.R. Du, preprint: cond-mat/0303472.
 - ¹² A.C. Durst, S. Sachdev, N. Read, and S.M. Girvin, preprint: cond-mat/0301569.
 - ¹³ A.V. Andreev, I.L. Aleiner, and A.J. Millis, preprint: cond-mat/0302063.
 - ¹⁴ P.W. Anderson and W.F. Brinkman, preprint: cond-mat/0302129.
 - ¹⁵ J. Shi and X.C. Xie, preprint: cond-mat/0302393.
 - ¹⁶ J.C. Phillips, preprint: cond-mat/0303181.
 - ¹⁷ A.A. Koulakov, and M.E. Raikh, preprint: cond-mat/0302465.
 - ¹⁸ V.I. Ryzhii, *Sov. Phys. Solid State* **11**, 2087 (1970).
 - ¹⁹ V.I. Ryzhii, R.A. Suris, and B.S. Shchamkhalova, *Sov. Phys.-Semicond.* **20**, 1299 (1986).
 - ²⁰ B.J. Keay, S. Zeuner, S.J. Allen, K.D. Maranowski, A.C. Gossard U. Bhattacharya, and M.J.W. Rodwell, *Phys. Rev. Lett.* **75**, 4102 (1995).
 - ²¹ P.K. Tien and J.P. Gordon, *Phys. Rev.* **129**, 647 (1963).
 - ²² X.L. Lei and S.Y. Liu, preprint: cond-mat/0304687.
 - ²³ M.G. Vavilov and I.L. Aleiner, preprint: cond-mat/0305478.
 - ²⁴ V. Ryzhii and V. Vyurkov, preprint: cond-mat/0305199.
 - ²⁵ V. Ryzhii, preprint: cond-mat/0305454.
 - ²⁶ V. Ryzhii, preprint: cond-mat/0305484.
 - ²⁷ V. Ryzhii and R. Suris, preprint: cond-mat/0307223.
 - ²⁸ S.Y. Liu and X.L. Lei, *J. Phys.: Condens. Matter*, **15** 4411 (2003).
 - ²⁹ X. L. Lei and C. S. Ting, *Phys. Rev. B* **32**, 1112 (1985).
 - ³⁰ X. L. Lei, J. L. Birman, and C. S. Ting, *J. Appl. Phys.* **58**, 2270 (1985) and the references therein.
 - ³¹ C. S. Ting, S. C. Ying, and J. J. Quinn, *Phys. Rev. B* **14**, 5394 (1977).
 - ³² X. L. Lei, *J. Appl. Phys.* **84**, 1396(1998); *J. Phys.: Condens. Matter* **10**, 3201 (1998).
 - ³³ A.D. Malov and V.I. Ryzhii, *Soviet Physics-Solid State*, **14**, 1766 (1973).
 - ³⁴ V.V. V'yurkov, A.D. Gladun, A.D. Malov, and V.I. Ryzhii, *Fiz. Tverd. Tela (Leningrad)* **19**, 3618 (1977).
 - ³⁵ T. Ando, A.B. Fowler, and F. Stern, *Rev. Mod. Phys.* **54**, 437 (1982).
 - ³⁶ D.R. Leadley, R.J. Nicholas, W. Xu, F.M. Peeters, J.T. Devreese, J. Singleton, J.A.A.J. Perenboom, I. van Bockstal, F. Herlach, C.T. Foxon, and J.J. Harris, *Phys. Rev. B* **48**, 5457 (1993).
 - ³⁷ V. Ryzhii and A. Satou, preprint: cond-mat/0306051.
 - ³⁸ Since at lattice temperature $T = 1$ K, the phonon contribution to magnetoresistivity is almost negligible, the impurity-induced resistivity $R_{xx}^{(i)}$ shown in Fig. 1 has only a minor difference from the total resistivity R_{xx} .